Geochemistry, Geophysics, Geosystems

METHOD

10.1029/2023GC010976

Key Points:

- An inlet system using inexpensive hardware and open-source software was developed for tunable infrared laser absorption spectroscopy
- Spectroscopic measurements of $\Delta'^{17}O$ in CO_2 can be negatively influenced by variable temperatures, uneven CO_2 mixing, which were addressed
- The external standard deviation of repeated $\Delta'^{17}O$ measurements of CO_2 from carbonates and air was better than 10 ppm

Supporting Information:

Supporting Information may be found in the online version of this article.

Correspondence to:

D. Bajnai,
david.bajnai@uni-goettingen.de

Citation:

Bajnai, D., Pack, A., Arduin Rode, F., Seefeld, M., Surma, J., & Di Rocco, T. (2023). A dual inlet system for laser spectroscopy of triple oxygen isotopes in carbonate-derived and air CO_2. *Geochemistry, Geophysics, Geosystems*, *24*, e2023GC010976. https://doi.org/10.1029/2023GC010976

Received 4 APR 2023
Accepted 25 SEP 2023

Author Contributions:

Conceptualization: David Bajnai, Andreas Pack
Data curation: David Bajnai
Formal analysis: David Bajnai
Funding acquisition: Andreas Pack
Investigation: David Bajnai, Fiorella Arduin Rode, Jakub Surma
Methodology: David Bajnai, Andreas Pack, Malte Seefeld, Tommaso Di Rocco
Software: David Bajnai, Andreas Pack, Malte Seefeld

A Dual Inlet System for Laser Spectroscopy of Triple Oxygen Isotopes in Carbonate-Derived and Air CO_2

David Bajnai[1], **Andreas Pack**[1], **Fiorella Arduin Rode**[1], **Malte Seefeld**[1], **Jakub Surma**[2], and **Tommaso Di Rocco**[1]

[1]Georg-August-Universität Göttingen, Geowissenschaftliches Zentrum, Göttingen, Germany, [2]Department of Earth and Planetary Sciences, Tokyo Institute of Technology, Meguro-ku Tokyo, Japan

Abstract Analyzing the triple oxygen isotope ($\Delta'^{17}O$) composition of carbonates and air CO_2 can provide valuable information about Earth system processes. However, accurately measuring the abundance of the rare ^{17}O-bearing CO_2 isotopologue using isotope ratio mass spectrometry presents significant challenges. Consequently, alternative approaches, such as laser spectroscopy, have been developed. Here, we describe an adaptable dual inlet system for a tunable infrared laser direct absorption spectrometer (TILDAS) that maintains stable instrumental conditions for subsequent sample and reference measurements. We report $\Delta'^{17}O$ measurements on three types of samples: reference CO_2, CO_2 derived from the acid digestion of carbonates, and air CO_2. The external repeatability ($\pm 1\sigma$) for reference-sample-reference bracketing measurements is generally better than ±10 ppm, close to the average internal error of ±6 ppm. Our results demonstrate that laser spectroscopy is a capable technique for measuring triple oxygen isotopes with the precision required to resolve variations in the $\Delta'^{17}O$ values of air CO_2 and to use the $\Delta'^{17}O$ of carbonates for paleothermometry.

Plain Language Summary Tunable infrared laser direct absorption spectroscopy (TILDAS) is a technique that determines isotopologue abundances by shining a laser through the analyzed gas and measuring the amount of light absorbed. Laser spectroscopy is emerging as a competitive alternative to the more common isotope ratio mass spectrometry due to its ability to provide rapid and precise measurements of rare isotope ratios directly on CO_2 gas. We present a cost-effective dual inlet system for TILDAS to measure the triple oxygen isotope composition of carbonates and air CO_2. Our setup maintains stable measurement conditions, for example, instrumental temperature, gas composition, pressure, and achieves external repeatability generally below ±10 ppm. Triple oxygen isotope measurements with such precision enable resolving variations in the ^{17}O-anomaly of air CO_2 and using the $\Delta'^{17}O$ values of carbonates for paleoenvironmental applications.

1. Introduction

The combined measurements of the three stable oxygen isotopes (^{16}O, ^{17}O, ^{18}O) is a valuable tool in Earth sciences to disentangle processes that traditional measurements of $^{18}O/^{16}O$ alone cannot distinguish (e.g., Miller & Pack, 2021; Pack & Herwartz, 2014). For instance, the triple oxygen isotope composition of air CO_2 informs on CO_2 sources and carbon exchange between atmospheric reservoirs (e.g., Hoag et al., 2005; Hofmann et al., 2017; Koren et al., 2019; Thiemens et al., 1995). Carbonate triple oxygen isotope measurements reveal the carbonate formation conditions and diagenetic alteration history and can be used to understand past hydrological processes (e.g., Affek et al., 2023; Bergel et al., 2020; Fosu et al., 2021; Kelson et al., 2022; Voarintsoa et al., 2020; Wostbrock, Brand, et al., 2020). These applications, however, require high-precision (uncertainties ≤10 ppm) triple oxygen isotope measurements of CO_2, which are labor-intensive and costly.

Variations in the triple oxygen isotope ratios are expressed using the δ-notation (Equation 1 for $\delta^{18}O$ in ‰; a similar equation can be written for $\delta^{17}O$; McKinney et al., 1950) and the $\Delta'^{17}O$ value (in ppm, Equation 2; Matsuhisa et al., 1978; Miller, 2002):

$$\delta^{18}O = \left(\frac{^{18}R_{\text{sample}}}{^{18}R_{\text{reference}}} - 1\right) \times 1000 \tag{1}$$

$$\Delta'^{17}O = 1000 \cdot \ln\left(\frac{\delta^{17}O}{1000} + 1\right) - \lambda_{\text{RL}} \times 1000 \cdot \ln\left(\frac{\delta^{18}O}{1000} + 1\right) \tag{2}$$

Visualization: David Bajnai
Writing – original draft: David Bajnai, Andreas Pack
Writing – review & editing: David Bajnai, Andreas Pack, Jakub Surma, Tommaso Di Rocco

In Equation 1, R represents the isotope ratio. In Equation 2, we choose $\lambda_{RL} = 0.528$ (cf., Luz & Barkan, 2010) to have a consistent terminology between the water and rock communities. In the following section, we refer to $10^3\ln(\delta^{17}O/10^3 + 1)$ and $10^3\ln(\delta^{18}O/10^3 + 1)$ as $\delta'^{17}O$ and $\delta'^{18}O$, respectively (cf., Miller, 2002; Miller & Pack, 2021).

While several studies have been published on the triple oxygen isotope composition of water (e.g., Aron et al., 2021; Barkan & Luz, 2005) and silicate rock samples (e.g., Pack & Herwartz, 2014), few studies have published high-precision triple oxygen isotope data on CO_2. This is because the isobaric interference from ^{13}C and ^{17}O substitutions within the CO_2 molecule hinders the direct isotope ratio mass spectrometric (IRMS) measurement of $\delta^{17}O$. The isotopologues $^{16}O^{13}C^{18}O$ and $^{17}O^{12}C^{18}O$ have nearly identical masses, and common IRMS techniques cannot resolve between the two (cf., Craig, 1957; Saenger et al., 2021).

Various alternative protocols have been developed to obtain the $\delta^{17}O$ value of CO_2. These include the high-temperature fluorination of CO_2 where $\Delta'^{17}O$ is analyzed on the resulting O_2 (Bhattacharya & Thiemens, 1989; Wostbrock, Brand, et al., 2020; Wostbrock, Cano, & Sharp, 2020), and high-temperature equilibration of CO_2 with CeO_2 or CuO (Assonov & Brenninkmeijer, 2001; Hofmann & Pack, 2010; Horváth et al., 2012; Kawagucci et al., 2005; Mahata et al., 2012; Mrozek et al., 2015), where the ^{17}O-anomaly is determined by mass-balance calculations. Barkan and Luz's (2012) approach includes the isotopic equilibration of CO_2 and H_2O followed by the fluorination of H_2O to O_2. In the protocols of Brenninkmeijer and Röckmann (1998) and Passey et al. (2014), CO_2 is first reduced with H_2 to CH_4 and H_2O, and then the $\delta^{17}O$ value of the water is analyzed using CoF_3 fluorination. Ellis and Passey (2023) built upon this methanation-fluorination technique, but the initial step of their method involves the high-temperature conversion of the oxygen in the analyzed material, for example, carbonates, to CO. Isotope exchange between CO_2 and O_2 over hot platinum is another established protocol to obtain high-precision $\Delta'^{17}O$ data (Adnew et al., 2022; Mahata et al., 2013). Limitations of these methods are that they are laborious and involve multiple fractionation steps, which can affect the accuracy of the results.

Alternatively, the $\delta^{17}O$ of CO_2 can be analyzed on the O^+ fragment ions using high-resolution gas source IRMS, which yields accurate and precise data but is time-consuming and costly (Adnew et al., 2019). Multi-collector secondary ion mass spectrometry of carbonates offers a high spatial resolution, but the precision for $\delta^{18}O$ and $\delta^{17}O$ is currently limited to ±0.5‰ (Bouden et al., 2021).

Laser absorption spectroscopy determines isotopologue abundances by detecting the absorbance of laser light by the analyte gas (McManus et al., 2006). Laser spectroscopy provides a quick and cost-effective approach for quantifying isotopologue ratios directly in CO_2 gas and has the potential to replace IRMS for many typical applications (Nelson et al., 2008; Prokhorov et al., 2019; Stoltmann et al., 2017; Tuzson et al., 2008; Wang et al., 2020; Yanay et al., 2022).

The first high-precision optical absorption measurements of ^{17}O anomalies in CO_2 were made using cavity-ring-down-spectroscopy (Stoltmann et al., 2017). Sakai et al. (2017) reported the first triple oxygen isotope analysis of CO_2 using tunable infrared laser direct absorption spectroscopy (TILDAS) with uncertainty for $\Delta'^{17}O$ of about 70 ppm. By improving the inlet system, Steur et al. (2021) subsequently reached 10–20 ppm precision. Hare et al. (2022) and Perdue et al. (2022) further improved the inlet system and published 5–19 ppm external precision ($\pm1\sigma$) for $\Delta'^{17}O$ measurements of carbonates, thereby showing that laser spectroscopy can attain the precision required for biogeochemical applications.

Ensuring identical analytical conditions for both sample and reference measurements is crucial in laser spectroscopy to minimize analytical bias. This is because the absorbance spectra—from which the isotope ratios are calculated—are influenced by factors such as temperature, pressure, and the partial pressure of the constituents in the analyte gas. The aim of this study was to present a cost-effective and fully automated inlet system for TILDAS that can measure the $\Delta'^{17}O$ of carbonate-derived and air CO_2 within 10 ppm.

2. The Dual Inlet System

2.1. Laser Spectrometer

Isotope analyses were conducted using the Aerodyne Research TILDAS fitted with a 0.16 L and 36 m multi-pass cell. The instrument was equipped with a distributed feedback interband cascade laser (Nanosystems and Technologies; 2905/22–26) emitting at 4256.6 nm. The laser driving current was modulated at 2.4 kHz, sweeping

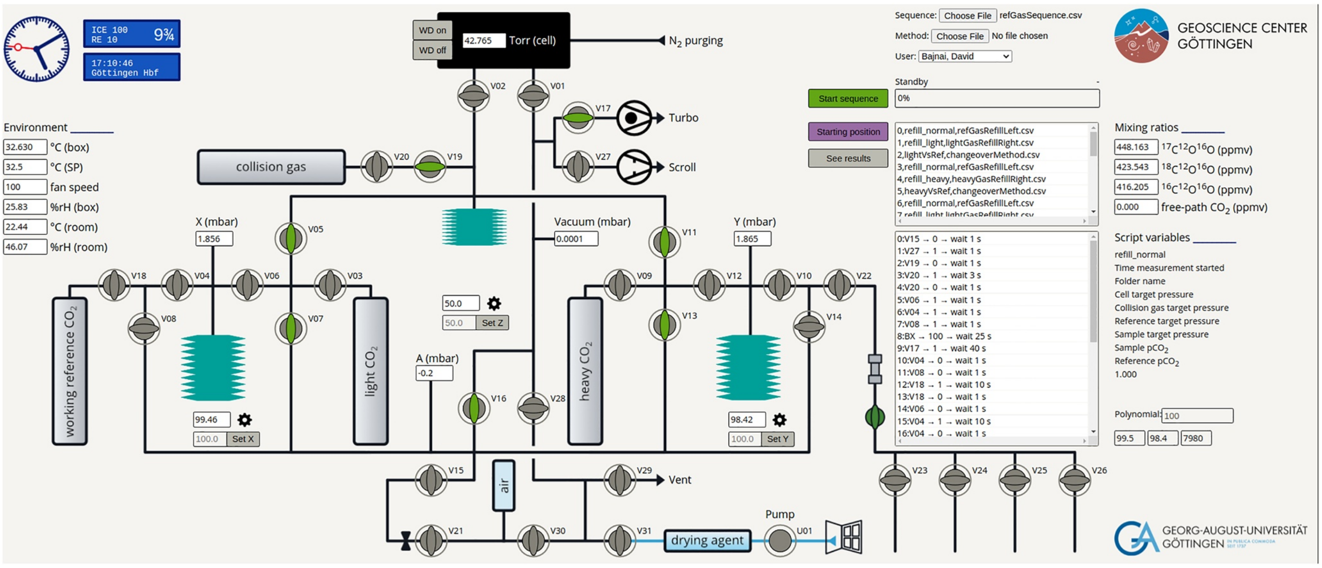

Sequence: Choose File refGasSequence.csv

Method: Choose File No file chosen

User: Bajnai, David

Standby -

0%

```
0,refill_normal,refGasRefillLeft.csv
1,refill_light,lightGasRefillRight.csv
2,lightVsRef,changeoverMethod.csv
3,refill_normal,refGasRefillLeft.csv
4,refill_heavy,heavyGasRefillRight.csv
5,heavyVsRef,changeoverMethod.csv
6,refill_normal,refGasRefillLeft.csv
7,refill_light,lightGasRefillRight.csv
```

```
0:V15 → 0 → wait 1 s
1:V27 → 1 → wait 1 s
2:V19 → 0 → wait 1 s
3:V20 → 1 → wait 3 s
4:V20 → 0 → wait 1 s
5:V06 → 1 → wait 1 s
6:V04 → 1 → wait 1 s
7:V08 → 1 → wait 1 s
8:BX → 100 → wait 25 s
9:V17 → 1 → wait 40 s
10:V04 → 0 → wait 1 s
11:V08 → 0 → wait 1 s
12:V18 → 1 → wait 10 s
13:V18 → 0 → wait 1 s
14:V06 → 0 → wait 1 s
15:V04 → 1 → wait 10 s
16:V04 → 0 → wait 1 s
```

Environment

32.630 °C (box)
32.5 °C (SP)
100 fan speed
25.83 %rH (box)
22.44 °C (room)
46.07 %rH (room)

42.765 Torr (cell)

X (mbar) 1.856

Vacuum (mbar) 0.0001

Y (mbar) 1.865

A (mbar) -0.2

50.0
50.0 Set Z

99.46
100.0 Set X

98.42
100.0 Set Y

Mixing ratios

448.163 $^{17}C^{12}O^{16}O$ (ppmv)
423.543 $^{18}C^{12}O^{16}O$ (ppmv)
416.205 $^{16}C^{12}O^{16}O$ (ppmv)
0.000 free-path CO_2 (ppmv)

Script variables

refill_normal
Time measurement started
Folder name
Cell target pressure
Collision gas target pressure
Reference target pressure
Sample target pressure
Sample pCO_2
Reference pCO_2
1.000

Polynomial: 100

99.5 98.4 7980

Figure 1. The front panel with a schematic diagram of the fully automated dual inlet system. The image is a screenshot of the graphical user interface, a website that runs within any internet browser.

across a ca. 50-nm-wide spectral window, and the transmitted light was recorded with a thermoelectrically cooled photovoltaic HgCdTe infrared detector (Teledyne Judson; J19). Spectral data were recorded at 1 Hz.

The single-laser setup resolved absorption peaks from the $^{16}O^{12}C^{16}O$ ("626"), $^{16}O^{12}C^{17}O$ ("627"), and $^{16}O^{12}C^{18}O$ ("628") CO_2 isotopologues. This shorthand notation for the isotopologues is widely used for laser-specific applications and is based on the spectroscopic high-resolution transmission molecular absorption database (HITRAN, Gordon et al., 2022).

The spectral fitting of our TILDAS instrument (see Section 3) was optimized for ca. 420 ppmv CO_2 in CO_2-free dry air to allow measurements of air CO_2 (cf., Bowling et al., 2003; Sturm et al., 2013). Consequently, prior to measurement, pure CO_2 samples had to be mixed with a collision gas. Because CO_2-free dry air was not readily available, we attempted to use other collision gases. First, we used pure Ar (Tyczka Industrie-Gase; Ar 4.6), which led to large spectral misfits. Switching to pure N_2 (Tyczka Industrie-Gase; N_2 3.5) showed a visible improvement in the spectral fit. Finally, on 13 September 2022, we changed to artificial, CO_2-free dry air (Air Products; 1.0 vol.% Ar, 20.9 vol.% O_2, 78.1 vol.% N_2).

The housing of the TILDAS was flushed with nitrogen to avoid the absorption of ambient CO_2 in the laser path. The dry purging gas was extracted from the headspace of a liquid nitrogen tank and was warmed up before being introduced to the TILDAS at a flow rate of ca. 2 L min^{-1}.

2.2. Hardware

The heart of the custom-built inlet system is a modified dual inlet system of a Finnigan MAT 251 mass spectrometer. The block containing the two bellows and the valves was extended with electropolished ¼-inch stainless steel tubings (Swagelok; 6L-T4-S-035-6M-E1) and pneumatically actuated bellows-sealed valves (Swagelok; SS-4BK-1C). We added a third bellow to the inlet system, constructed from a bellows-sealed corner valve with ISO-KF 16 connectors. The system is connected to a dry scroll pump (Edwards; nXDS6i) and a turbomolecular pump (Pfeiffer Vacuum; HiPace 80) via an ISO-KF 25 flexible stainless-steel hose, allowing it to reach a $\leq 10^{-4}$ mbar vacuum in the setup (Figure 1).

The inlet system is operated by a Raspberry Pi mini-computer (Raspberry Pi 4 Model B Rev 1.1 4GB). Besides communicating with the Windows PC of the TILDAS, the Raspberry Pi controls an Arduino (Arduino MEGA 2560 Rev3) microcontroller, which interfaces with the valves, relays, the stepper motors for bellow positioning, and connected sensors (Figure S1 in Supporting Information S1). On receiving a command from the Raspberry Pi, the Arduino opens and closes the pneumatic valves of the inlet system using Darlington drivers (STMicro;

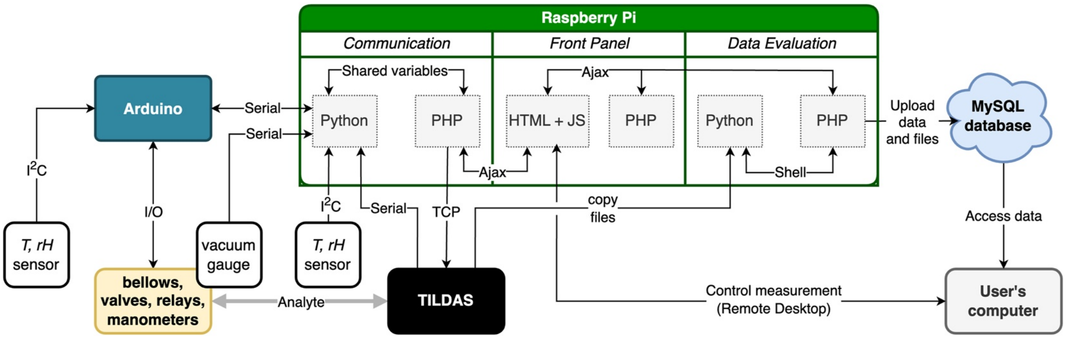

Figure 2. An overview of the relationships between the dual inlet software and hardware.

ULN2803A) and solenoid valve actuators (SMC; V100 series). The Arduino expands and compresses the bellows using NEMA17 stepper motors controlled by DRV8825 (Texas Instruments) drivers. The peristaltic pump (Grothen; G528, 12 V, 3 × 5 mm) of the air inlet system is turned on and off using a 5 V relay.

Two capacitance manometers (MKS Instruments; Baratron 623H, 10 Torr) are used to measure the CO_2 pressure in the bellows, while the pressure of the collision gas (gauge A on Figure 1) is measured by a third manometer (MKS Instruments; Baratron 626B, 1,000 mbar). Because the manometers produce a 0–10 V output signal that is read by the Arduino's 0–5 V analog in ports, only pressures below 5 Torr and 500 mbar are recorded, respectively. To increase the resolution of the readings, pressure data are averaged over 1 s intervals. The pressure in the absorption cell is measured using the TILDAS's built-in capacitance manometer (MKS Instruments; Baratron 722B, 100 Torr). An active Pirani gauge measures the vacuum in the inlet system (Edwards; APG100-XLC, $10^{-4} \leq p \leq 10^{3}$ mbar).

For thermal stability during the measurements, the TILDAS and its peripherals, including the chiller (Solid State Cooling Systems; Oasis Three) and the inlet system, are placed in a 5-cm-thick styrofoam-insulated wooden box. The temperature inside the box is measured using an SHTC3 sensor (Adafruit Industries) connected to the Arduino via I^2C, and regulated to 32.00°C (±0.01°C; $\pm 1\sigma$ of the temperature data over a ca. 2.5-hr-long measurement; Figures S3g and S6g in Supporting Information S1) using two 80 mm housing fans, which blow cool (ca. 25°C) laboratory air into and ventilate warm air out of the box, respectively (see Section 4.1). Specifically, the speed (i.e., the current) of the fans is PID-controlled by the Arduino and an adjustable power supply (Manson, HCS-3304). The ambient temperature outside the housing was monitored using a BME688 (Pimoroni) sensor connected to the Raspberry Pi via I^2C.

2.3. Software

The inlet system is operated by open-source software. The measurement procedure is controlled via the front panel (Figure 1), a JavaScript web application running on the Raspberry Pi (Figure 2). An Apache HTTP server provides the browser front end. We run the web application within the browser of the Raspberry Pi and access it via Microsoft Remote Desktop.

Information exchange between the JavaScript web application and the hardware interfaces is done in two steps via a Python (v. 3.7) and a PHP (v. 8.2) script (Figure 2). A continuously looping Python program (ca. 12 Hz) receives a status string from the Arduino (valve status, position of the bellows, pressure data, etc.) and sends back commands (actuating valves, moving bellows, etc.) via serial. The PHP script exchanges data with the Python script via shared variables, and the JavaScript web application via AJAX calls.

The Aerodyne Research TDLWintel software on the TILDAS PC controls the laser spectrometer and performs the spectra fitting. The TILDAS PC is run headless but can be accessed via the Remote Desktop if necessary. The TDLWintel software sends status strings containing the measured isotopologue mixing ratios and the cell pressure to the Raspberry Pi via serial. It receives commands, that is, to start or stop saving spectral data, from the TILDAS through TCP via a PHP script (Figure 2). Clock synchronization between the TILDAS PC and the Raspberry Pi was achieved using a shared local time server.

When a measurement is finished, the saved STC and STR files (containing the mixing ratios, among other information) are copied from the TILDAS PC to the Raspberry Pi. A Python script reads these files and uses them for data reduction (Figure 2). Finally, all data files and the evaluated results are uploaded to a MySQL database, which can be accessed online.

2.4. Gas Mixing and Inlet

The entire gas mixing and admission procedure is automated. The sequence of commands is stored in CSV files read by the JavaScript web application. For carbonate-derived CO_2 samples, a manifold containing the sample CO_2 gas is connected to the inlet system via an UltraTorr connector (behind V22; Figure 1). The pneumatic valves of the manifold are actuated automatically during sample bellow refill. To refill the reference bellows, aliquots of the reference CO_2 are taken automatically from tanks placed inside the housing and connected to the inlet system via stainless-steel capillaries. The pure CO_2 gas (sample and reference) is mixed with the collision gas before expansion into the absorption cell. First, the sample or reference CO_2 is expanded into a small volume (for the reference, the cross-piece enclosed by V3, V5, V6, V7; and for the sample V9, V11, V12, V13; Figure 1). The pressure in these volumes is adjusted by moving bellows *X* and *Y*, respectively. The collision gas is first expanded to the volume enclosed by V19 and V20 before an aliquot is expanded to the volume between valves V07, V08, V13, V14, V15, and V16. The amount of collision gas is adjusted by moving bellow *Z*. The pure CO_2 and the collision gas are mixed turbulently by first expanding the collision gas into the cross-piece holding the CO_2 (opening V7 for reference or V13 for sample) and then expanding the analyte to the absorption cell. With this procedure, the mixing ratio (pCO_2; here, the concentration of the "626" isotopologue; ca. 420 ppmv) can be adjusted to better than ±0.5 ppmv for reference-sample pairs (Figures S3c, S6c, and S11c in Supporting Information S1). Finally, the pressure in the cell was adjusted using bellow *Z* to ca. 42.100 Torr. For a single measurement, sample and reference analyte pressures are matched within ±0.002 Torr (Figures S3d, S6d, and S9d in Supporting Information S1). The mixing and gas changeover takes approximately 4 min.

The inlet system allows the automated sampling of ambient air by pumping it from outside the laboratory using a peristaltic pump throughout a 6 mm polyurethane tube at a rate of approximately 0.2 L min^{-1} (V32; Figure 1). Water vapor has a considerable peak-broadening effect (Tan et al., 2019). Since air humidity is highly variable, it is necessary to dry the air to maintain a consistent analyte composition across multiple measurements. For this reason, the air is passed through a 1-cm-inner-diameter and 20-cm-long glass tube containing a drying agent and subsequently a 0.5 μm filter. Although we used coarse anhydrous magnesium perchlorate during the test measurements, other methods, such as a Nafion gas dryer, may be more suitable for drying the sample without affecting its isotopic composition (cf., Paul et al., 2020). To flush the line before sampling, fresh air is pumped through the polyurethane tubing and the drying agent. Then, a ca. 1 L volume between V30 and V21 was filled with air for 5 min. By opening V15 and V21, the volume between valves V07, V08, V13, V14, and V16 is slowly filled to a pre-set target pressure through a crimped capillary. The pCO_2 of the air sample is recorded after it is expanded into the optical cell, which allows automatic adjustment of the mixing ratio of the reference gas during the following measurement cycle.

2.5. Sample Material

To test the repeatability and stability of the instrument, we report data from two pure CO_2 gases, a speleothem calcite sample, and air CO_2. Pure CO_2 gases were taken from gas bottles connected to the inlet system (Figure 1). The "light CO_2" ($\delta^{18}O = -0.92‰$ VSMOW was produced by equilibrating CO_2 with isotopically light Antarctic precipitates. The "heavy CO_2" ($\delta^{18}O = 77.03‰$ VSMOW) was equilibrated with isotopically heavy water that remained after evaporating tap water.

CO_2 was extracted from a speleothem calcite sample offline using acid digestion with phosphoric acid at 25°C. For each extraction, ca. 2 mg of carbonate powder reacted overnight with >103% phosphoric acid in an inverse Y-shaped reactor vessel (McCrea, 1950). The liberated CO_2 was purified using a −80°C ethanol slush trap and frozen out in the sample manifold.

Air for the automated air CO_2 measurements was collected from the fourth floor balcony of the stable isotope laboratory in Göttingen, Germany.

3. Data Reduction

During an approximately 4-min-long measurement cycle, the oxygen isotope ratios of the analyte are calculated every second. Specifically, the TDLWintel software calculates mole fractions (X; also referred to as mixing ratios) of the three investigated molecular species ("626," "627," and "628") from the absorption spectra through spectral fitting (McManus et al., 2006). For the spectral fitting, the concentration of the "free-path CO_2" species in the TDLWintel was set to zero. The isotope ratios (R) are calculated from the mole fractions (Equation 3):

$$^{17}R = \frac{\chi_{627}}{\chi_{626}} \quad ^{18}R = \frac{\chi_{628}}{\chi_{626}} \tag{3}$$

To calculate isotope deltas, the isotope composition of the sample CO_2 was compared with the isotope composition of the reference. We tested two data reduction approaches to address instrumental drift: "reference-sample-reference bracketing" and "smooth drift correction." In the case of each approach, for a replicate analysis, we measure reference and sample cycles consecutively multiple times. The first "dummy" measurement cycle is always discarded because it often deviates from the subsequent reference cycles. A 3σ outlier test is performed on the ca. 240 data points in each measurement cycle.

The traditional way of calculating isotope ratios is to bracket sample measurement cycles between reference cycles, with quick changeovers in-between (McKinney et al., 1950). A replicate measurement consists of an odd number of gas analysis cycles, with the odd cycles reserved for reference gas measurements and the even cycles used for sample gas measurements (Figures S4 and S10 in Supporting Information S1). This technique accounts for the instabilities of the instrument by comparing the isotope ratio R (Equation 3) of the sample with the mean isotope ratio of a reference that is measured, presumably, under the same conditions immediately before and after the sample:

$$\delta^{\text{sample}}_{\text{working gas}} = \sum_{\substack{i=2 \\ i\epsilon 2\mathbb{N}}}^{\substack{n-1 \\ n\epsilon 2\mathbb{N}+1}} \left[\left(\frac{R^{\text{working gas}}_{i-1} + R^{\text{working gas}}_{i+1}}{2R^{\text{sample}}_{i}} - 1 \right) \times 1000 \right] \frac{2}{n-1} \tag{4}$$

For our "bracketing" analyses, we measured a total of $n = 21$ cycles. The internal error of the "bracketing" replicate is calculated as the 1 standard error of the $\Delta'^{17}O$ values of the cycles (Figures S5 and S11 in Supporting Information S1).

The drift of the instrument, however, may follow a smooth path, for example, in the form of a sinusoid function. While the bracketing approach can deal with such a situation, it is not the correct mathematical description. Instead, the reference and sample would follow a parallel trend with a constant offset in the intercept. One could approximate the sinusoid drift by fitting polynomial models with identical coefficients but unique intercepts to all sample and reference data points. The difference in the intercepts of the two polynomial fit models provides an apparent isotope fractionation factor (α) from which the raw isotope ratios are calculated.

For a "smooth drift" replicate, we measured two sample cycles interspersed with reference cycles and fitted a second-order polynomial model on the data (Figures S6 and S7 in Supporting Information S1). Our initial testing showed that measuring more than two sample cycles hindered a satisfactory polynomial fit of any degree, due to the rapid and non-linear drift of the measurements (see Section 4.1). The internal error of the "smooth drift" measurements was calculated by taking the root mean squared standard deviations of the differences in $\Delta'^{17}O$ between the polynomial models and the reference or sample data points.

The isotope compositions referenced against a working gas are typically recalculated relative to an international standard. However, the $\delta^{17}O$ value of our working reference gas is unknown. As a working reference gas, we use a commercial CO_2 (Linde Gas; CO_2 4.5) with a $\delta^{18}O$ value of 27.87‰ VSMOW. Although a nominal $\Delta'^{17}O$ value of −90 ppm was assigned to our working reference based on high-resolution gas source mass spectrometry (cf., Adnew et al., 2019), we only report unreferenced and unscaled isotope ratios.

4. Sensitivity of the $\Delta'^{17}O$ Measurements

4.1. Effect of Temperature Instability

Initially, we placed the TILDAS and the inlet system in an air-conditioned laboratory with a temperature instability of ca. 1.5°C h^{-1}. This led to a considerable 1,400 ppm fluctuation in the measured $\Delta'^{17}O$ values over an 8-hr interval (Figure 3).

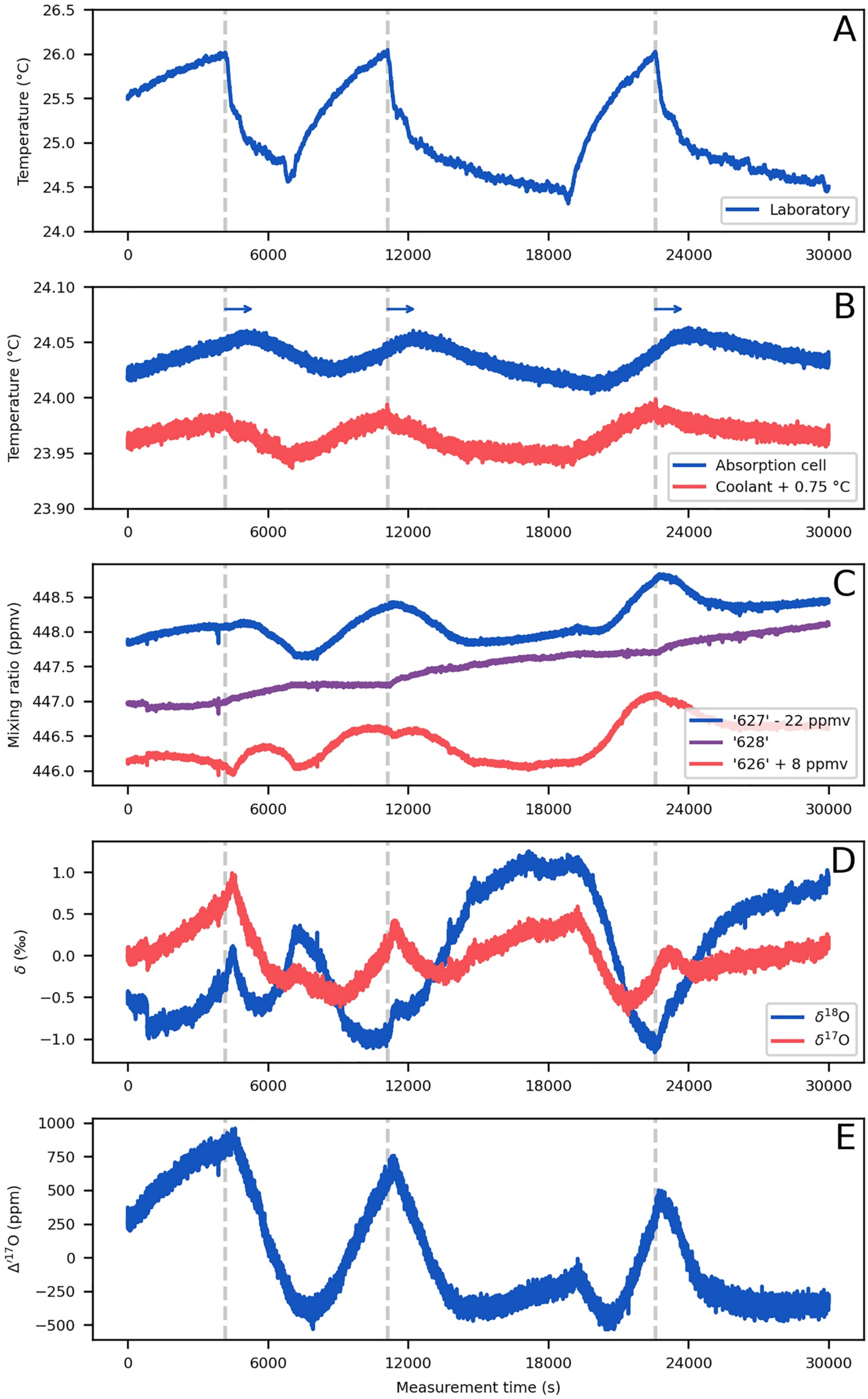

Figure 3. The effect of changing ambient temperatures on the measured isotope ratios. The fluctuating room temperature (a, $\Delta T \approx 1.5$°C) is mirrored (b, $\Delta T \approx 0.06$°C) in the coolant and with a lag ($\Delta t = 20$ min, blue arrows) in the cell temperatures. Variations in the cell temperatures led to uncorrelated variations in the measured mixing ratios (c) and the δ-values (d). The Δ'^{17}O (e) roughly follows the changing cell temperature and shows variations of approximately 1,400 ppm.

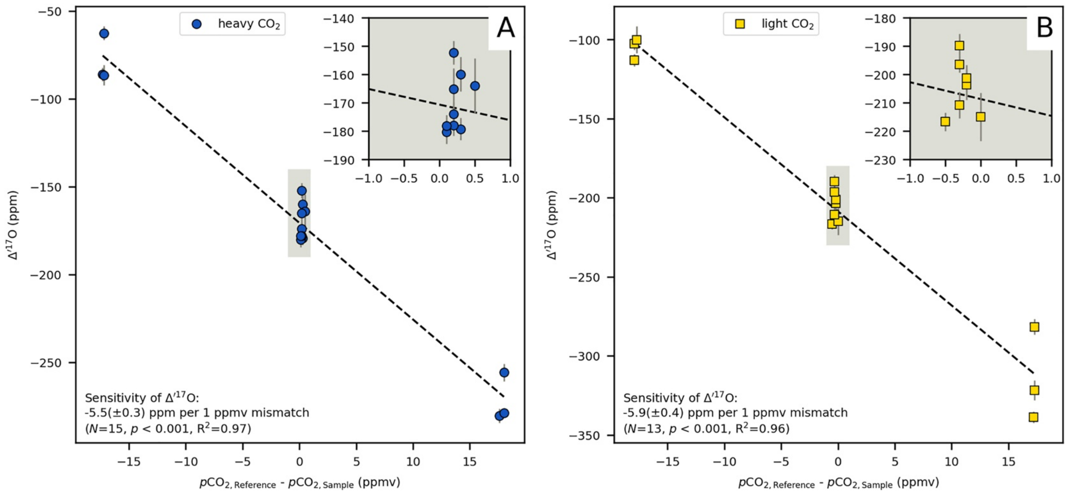

Figure 4. Sensitivity of the $\Delta'^{17}O$ values to the mismatch between the sample and reference analyte's pCO_2.

The 1.5°C h^{-1} variation in ambient room temperature caused by the air conditioning (Figure 3a) was inherited by the coolant and cell temperatures, varying, in turn, by ca. 0.06°C h^{-1} (Figure 3b). Although the coolant temperature was in phase with the ambient room temperature, the cell temperature showed about 20 min lag because of the buffering effect of the hardware around the cell's temperature sensor (Figure 3b). Previous studies have also noted the detrimental effects of unstable cell and electronics hardware temperatures on the repeatability of the $\Delta'^{17}O$ measurements by laser spectroscopy (Bowling et al., 2003; Hare et al., 2022; Stoltmann et al., 2017).

Although the intensities of the absorption lines resembled the variability in the cell temperature (Figure 3c), the absorbance of the three isotopologues exhibited different sensitivities to temperature changes (Figure S2 in Supporting Information S1). This irregular behavior resulted in uncorrelated variations in $\delta^{17}O$ and $\delta^{18}O$ (Figure 3d), which funneled into the large approximately 1,400 ppm variations in $\Delta'^{17}O$ (Figure 3e). The observed non-linear short-scale drift could not be handled by either correction method. Attempts to apply a cell temperature-based correction proved challenging, likely because the measured temperature does not precisely match the actual gas temperature.

Instead, we aimed to minimize temperature fluctuations. Placing the TILDAS and the inlet system in an insulated box equipped with active temperature control (see Section 2.2) led to stable cell temperatures (±2 mK over a ca. 2.5-hr-long measurement) and consequently a dramatically reduced drift in the isotope ratios (Figures S3, S6, and S9 in Supporting Information S1). The remaining drift could be effectively managed by frequent sample-reference changeovers.

4.2. Effect of pCO_2 Mismatch

We noticed that a mismatch between the reference and the sample analyte's pCO_2—introduced by inaccurate mixing of CO_2 and collision gas—influenced the $\Delta'^{17}O$ measurements. Perdue et al. (2022) also investigated the impact of pCO_2 mismatch but found no decipherable effect within ±25 ppmv (see their Figure 8). To investigate this for our setup, a series of heavy and light CO_2 measurements were taken with intentionally introduced mixing ratio mismatch while maintaining the overall cell pressure constant. The data were evaluated using the "bracketing" approach.

Our results show a clear negative correlation between the measured $\Delta'^{17}O$ values and the magnitude of the pCO_2 mismatch, with a slope of ca. −6 ppm $ppmv^{-1}$ (Figure 4). For the heavy and light CO_2 measurements, where the sample and reference pCO_2 were precisely matched, the average internal error was approximately ±5 ppm (Figure 4 insets). Consequently, a pCO_2 mismatch larger than ±1 ppmv would introduce a bias larger than the internal error.

We opted to minimize the pCO_2 mismatch during gas mixing rather than correcting the measured data. Thanks to our fully automated inlet system, achieving pressure matching at a level where pCO_2 mismatches are negli-

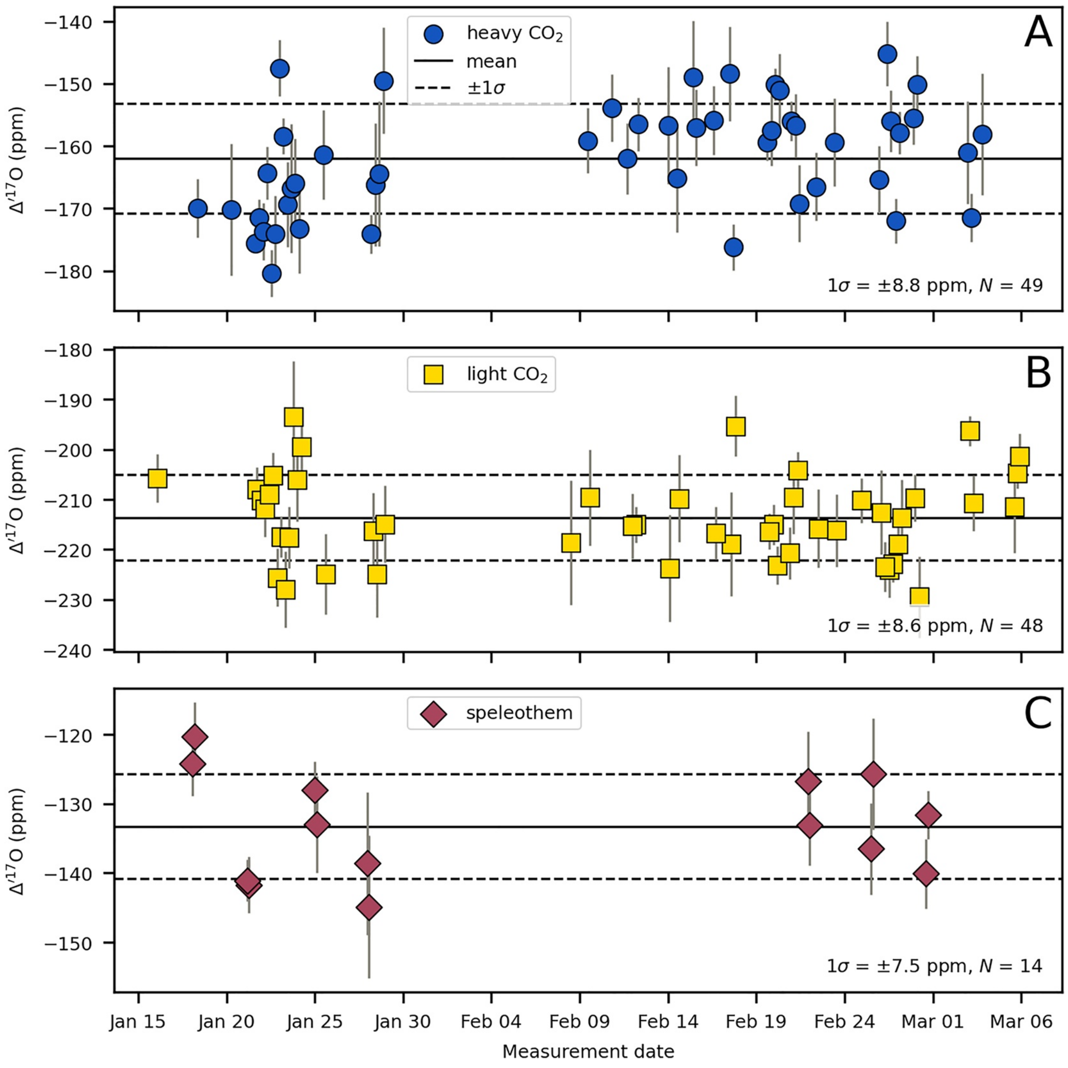

Figure 5. Triple oxygen isotope measurements evaluated using the "bracketing" approach. $\Delta'^{17}O$ data from two CO_2 gases (a), (b) and a carbonate (c), relative to the working reference gas.

gible (i.e., better than ±0.5 ppmv) was a straightforward task involving just a few lines of code. Additionally, since pressure matching takes place simultaneously with the measurement, this procedure does not introduce any delays into the measurement sequence.

5. Repeatability of $\Delta'^{17}O$

5.1. Analysis of Pure CO_2 Mixed With Collision Gas

To demonstrate the long-term repeatability of each data reduction approach, we report $\Delta'^{17}O$ data from two measurement periods. We tested the "smooth drift" approach first as it offered a short measurement time for a single replicate analysis (ca. 40 min; Figures S6 and S7 in Supporting Information S1). The internal error of the "smooth drift" measurements was ca. ±4 ppm, whereas the external repeatability (±1σ) over a ca. two-week period was ca. ±15 ppm (Figure S8 in Supporting Information S1). For the "bracketing" measurements (e.g., Figures S3–S5 in Supporting Information S1), the external repeatability of the data (±1σ) over a ca. one-month period was ±9 ppm, while the mean internal error was ±6 ppm (Figures 5a and 5b). The reason why the "smooth drift" approach performs worse than "bracketing" is probably because the instrument, despite the temperature stabilization, drifts at a faster rate than what a polynomial fit can accurately track.

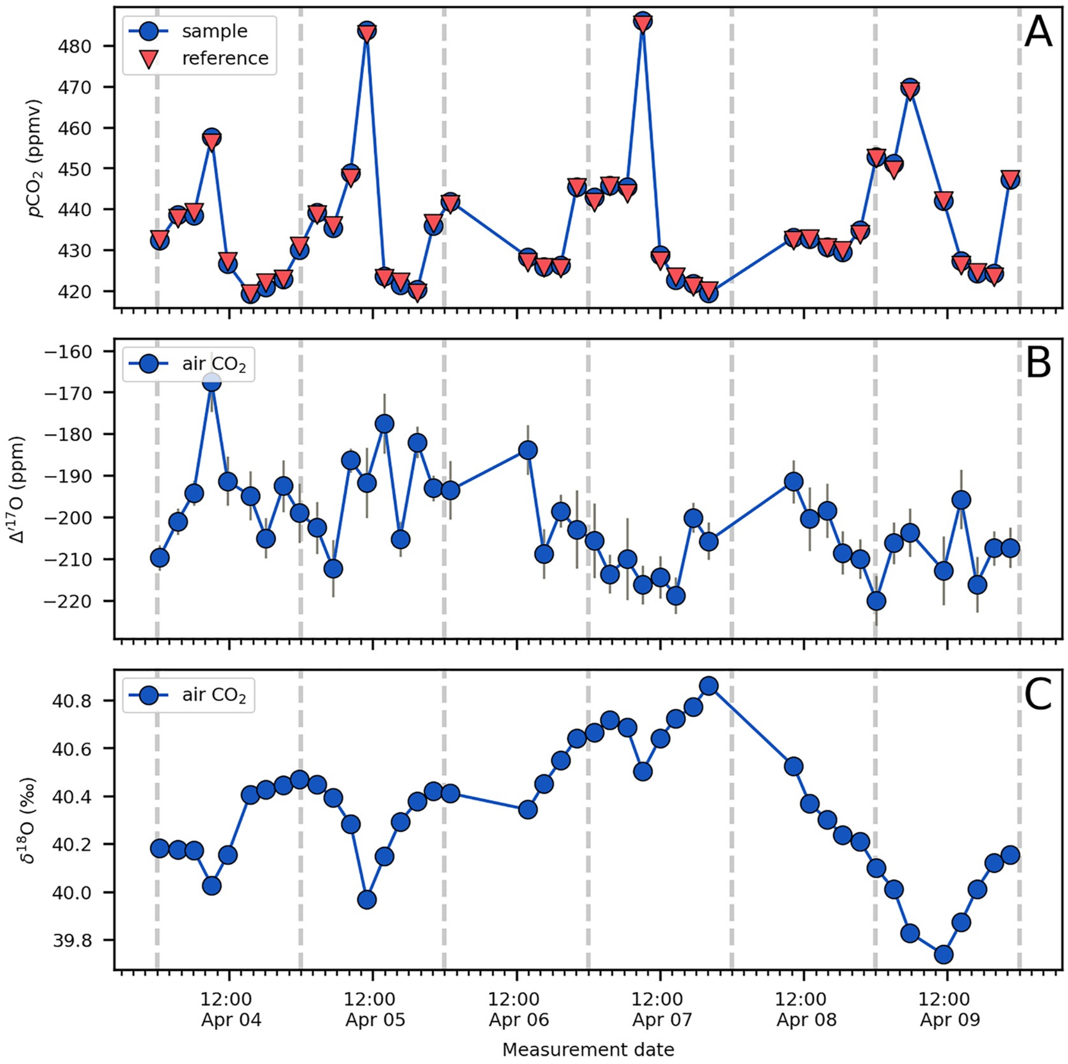

Figure 6. Results of automated air CO_2 measurements. (a) Cell pCO_2 averaged for the eight sample and nine reference cycles in each replicate measurement. (b) $\Delta'^{17}O$ values of air CO_2, referenced against the working gas. (c) $\delta^{18}O$ values of air CO_2, referenced against the working gas.

Despite the large difference in the $\delta^{18}O$ values between the light and heavy CO_2, neither data reduction approach shows a resolvable drift in the $\Delta'^{17}O$ values (Figures 5a and 5b; Figure S8 in Supporting Information S1). This suggests that if instrumental conditions (e.g., cell temperature) are stable, the scale compression (i.e., the difference in the δ-values) of the instrument does not change rapidly. Once their isotope composition is accurately determined, the light and heavy reference CO_2 can be used for scaling the data.

Because the "bracketing" approach resulted in better external repeatability, we used it for evaluating speleothem measurements (Figure 5c). A total of 14 analyses of carbonate-derived CO_2 were performed, obtained from seven acid digestions, that is, each aliquot was analyzed twice. The analyses yielded an external repeatability of ±8 ppm (±1σ).

Our system has an external $\Delta'^{17}O$ repeatability of ±8–9 ppm (±1σ), which is comparable to that reported by Perdue et al. (2022) and Hare et al. (2022), who used similar TILDAS systems. Our studies demonstrate that laser spectroscopy yields similar or better repeatability than more time-intensive and expensive methods (Adnew et al., 2019; Fosu et al., 2020; Passey et al., 2014; Wostbrock, Cano, & Sharp, 2020).

5.2. Analyses of Air CO_2

The concentration of atmospheric CO_2 can fluctuate by as much as 100 ppmv due to variations in urban CO_2 fluxes and vegetation uptake (e.g., George et al., 2007; Hofmann et al., 2017). Consequently, continuous monitoring requires adjusting the $p$$CO_2$ of the reference gas mixture to match the ambient air $p$$CO_2$ (Figure 6a). To achieve this, we used a modified "bracketing" measurement procedure, where the amount of working gas mixed with collision gas was automatically adjusted based on the pCO2 of the first air cycle. The first three measurement cycles (dummy and two adjustment cycles) were discarded (Figures S9–S11 in Supporting Information S1).

The mean internal error of the air CO_2 $\Delta'^{17}O$ measurements was similar to that of pure CO_2 mixed with collision gas, that is, ±6 ppm (Figure 6b). Compared to CeO_2 equilibration (Hofmann et al., 2017) and high-temperature fluorination (Thiemens et al., 2014), laser spectroscopy offers a three-fold improvement in precision. In addition, rapid, consecutive measurements of air CO_2 can potentially resolve daily variations in its $\Delta'^{17}O$ value, opening new avenues for atmospheric research (Figure 6).

6. Conclusions

We present an adaptable, fully automated dual inlet system for tunable infrared laser direct absorption spectroscopy (TILDAS) that uses inexpensive hardware and open-source software. The setup implements the identical treatment of sample and reference by accurately mixing the analyte CO_2 with collision gas before each analysis cycle, and thereby allows high-precision ($1\sigma \leq 10$ ppm) triple oxygen isotope ($\Delta'^{17}O$) measurements of pure CO_2 (e.g., from acid digestion of carbonates) and air CO_2. By matching the reference gas mixing ratios to that of ambient air, the setup enables the continuous monitoring of the triple oxygen isotope composition of air CO_2. Our study shows that laser spectroscopy can generate high-precision data for Earth system applications, provided that sample and reference measurements are conducted under identical conditions.

Data Availability Statement

The source code of the inlet system described in this manuscript can be downloaded from GitHub (https://github.com/davidbajnai/TARDIS) and Zenodo (Bajnai & Pack, 2023). All data presented in this paper are deposited in the same repositories.

Acknowledgments
The authors thank Dennis Kohl, Axel Dierschke, Thierry Wasselin, Swea Klipsch, and Oliver Jäger for their technical help in the laboratory. The authors would also like to express their appreciation to Christoph Dyroff (Aerodyne Research) for his assistance with the initial setup of the TILDAS. Andreas Pack acknowledges the funding of the TILDAS instrument by the University of Göttingen. The authors thank the Centre for Stable Isotope Research and Analysis, University of Göttingen, for providing hardware parts for the inlet system. Open Access funding enabled and organized by Projekt DEAL.

References

Adnew, G. A., Hofmann, M. E. G., Paul, D., Laskar, A., Surma, J., Albrecht, N., et al. (2019). Determination of the triple oxygen and carbon isotopic composition of CO_2 from atomic ion fragments formed in the ion source of the 253 Ultra high-resolution isotope ratio mass spectrometer. *Rapid Communications in Mass Spectrometry*, *33*(17), 1363–1380. https://doi.org/10.1002/rcm.8478

Adnew, G. A., Workman, E., Janssen, C., & Röckmann, T. (2022). Temperature dependence of isotopic fractionation in the CO_2-O_2 isotope exchange reaction. *Rapid Communications in Mass Spectrometry*, *36*(12). https://doi.org/10.1002/rcm.9301

Affek, H. P., Vieten, R., Barkan, E., Levi, Y., Ayalon, A., Bar-Matthews, M., et al. (2023). $^{17}O_{excess}$ in speleothem carbonates in Soreq Cave as an archive for hydro-climatic conditions. *Earth and Planetary Science Letters*, *621*, 118366. https://doi.org/10.1016/j.epsl.2023.118366

Aron, P. G., Levin, N. E., Beverly, E. J., Huth, T. E., Passey, B. H., Pelletier, E. M., et al. (2021). Triple oxygen isotopes in the water cycle. *Chemical Geology*, *565*, 116770. https://doi.org/10.1016/j.chemgeo.2020.120026

Assonov, S. S., & Brenninkmeijer, C. A. M. (2001). A new method to determine the ^{17}O isotopic abundance in CO_2 using oxygen isotope exchange with a solid oxide. *Rapid Communications in Mass Spectrometry*, *15*(24), 2426–2437. https://doi.org/10.1002/rcm.529

Bajnai, D., & Pack, A. (2023). TARDIS: TILDAS + automated remix & dual inlet system (v2.0) [Dataset]. Zenodo. https://doi.org/10.5281/zenodo.8139075

Barkan, E., & Luz, B. (2005). High precision measurements of $^{17}O/^{16}O$ and $^{18}O/^{16}O$ ratios in H_2O. *Rapid Communications in Mass Spectrometry*, *19*(24), 3737–3742. https://doi.org/10.1002/rcm.2250

Barkan, E., & Luz, B. (2012). High-precision measurements of $^{17}O/^{16}O$ and $^{18}O/^{16}O$ ratios in CO_2. *Rapid Communications in Mass Spectrometry*, *26*(23), 2733–2738. https://doi.org/10.1002/rcm.6400

Bergel, S. J., Barkan, E., Stein, M., & Affek, H. P. (2020). Carbonate $^{17}O_{excess}$ as a paleo-hydrology proxy: Triple oxygen isotope fractionation between H_2O and biogenic aragonite, derived from freshwater mollusks. *Geochimica et Cosmochimica Acta*, *275*, 36–47. https://doi.org/10.1016/j.gca.2020.02.005

Bhattacharya, S. K., & Thiemens, M. H. (1989). Effect of isotopic exchange upon symmetry dependent fractionation in the $O + CO \rightarrow CO_2$ reaction. *Zeitschrift Für Naturforschung A*, *44*(9), 811–813. https://doi.org/10.1515/zna-1989-0906

Bouden, N., Villeneuve, J., Marrocchi, Y., Deloule, E., Füri, E., Gurenko, A., et al. (2021). Triple oxygen isotope measurements by multi-collector secondary ion mass spectrometry. *Frontiers in Earth Science*, *8*, 601169. https://doi.org/10.3389/feart.2020.601169

Bowling, D. R., Sargent, S. D., Tanner, B. D., & Ehleringer, J. R. (2003). Tunable diode laser absorption spectroscopy for stable isotope studies of ecosystem–atmosphere CO_2 exchange. *Agricultural and Forest Meteorology*, *118*(1–2), 1–19. https://doi.org/10.1016/S0168-1923(03)00074-1

Brenninkmeijer, C. A. M., & Röckmann, T. (1998). A rapid method for the preparation of O_2 from CO_2 for mass spectrometric measurement of $^{17}O/^{16}O$ ratios. *Rapid Communications in Mass Spectrometry*, *12*(8), 479–483. https://doi.org/10.1002/(SICI)1097-0231(19980430)12:8<479::AID-RCM184>3.0.CO;2-R

Craig, H. (1957). Isotopic standards for carbon and oxygen and correction factors for mass-spectrometric analysis of carbon dioxide. *Geochimica et Cosmochimica Acta*, *12*(1–2), 133–149. https://doi.org/10.1016/0016-7037(57)90024-8

Ellis, N. M., & Passey, B. H. (2023). A novel method for high-precision triple oxygen isotope analysis of diverse Earth materials using high temperature conversion–methanation–fluorination and isotope ratio mass spectrometry. *Chemical Geology*, *635*, 121616. https://doi.org/10.1016/j.chemgeo.2023.121616

Fosu, B. R., Ghosh, P., Weisenberger, T. B., Spürgin, S., & Viladkar, S. G. (2021). A triple oxygen isotope perspective on the origin, evolution, and diagenetic alteration of carbonatites. *Geochimica et Cosmochimica Acta*, *299*, 52–68. https://doi.org/10.1016/j.gca.2021.01.037

Fosu, B. R., Subba, R., Peethambaran, R., Bhattacharya, S. K., & Ghosh, P. (2020). Technical Note: Developments and applications in triple oxygen isotope analysis of carbonates. *ACS Earth and Space Chemistry*, *4*(5), 702–710. https://doi.org/10.1021/acsearthspacechem.9b00330

George, K., Ziska, L. H., Bunce, J. A., & Quebedeaux, B. (2007). Elevated atmospheric CO_2 concentration and temperature across an urban–rural transect. *Atmospheric Environment*, *41*(35), 7654–7665. https://doi.org/10.1016/j.atmosenv.2007.08.018

Gordon, I. E., Rothman, L. S., Hargreaves, R. J., Hashemi, R., Karlovets, E. V., Skinner, F. M., et al. (2022). The HITRAN2020 molecular spectroscopic database. *Journal of Quantitative Spectroscopy and Radiative Transfer*, *277*, 107949. https://doi.org/10.1016/j.jqsrt.2021.107949

Hare, V. J., Dyroff, C., Nelson, D. D., & Yarian, D. A. (2022). High-precision triple oxygen isotope analysis of carbon dioxide by tunable infrared laser absorption spectroscopy. *Analytical Chemistry*, *94*(46), 16023–16032. https://doi.org/10.1021/acs.analchem.2c03005

Hoag, K. J., Still, C. J., Fung, I. Y., & Boering, K. A. (2005). Triple oxygen isotope composition of tropospheric carbon dioxide as a tracer of terrestrial gross carbon fluxes. *Geophysical Research Letters*, *32*(2), L02802. https://doi.org/10.1029/2004GL021011

Hofmann, M. E., & Pack, A. (2010). Technique for high-precision analysis of triple oxygen isotope ratios in carbon dioxide. *Analytical Chemistry*, *82*(11), 4357–4361. https://doi.org/10.1021/ac902731m

Hofmann, M. E. G., Horváth, B., Schneider, L., Peters, W., Schützenmeister, K., & Pack, A. (2017). Atmospheric measurements of Δ^{17}O in CO_2 in Göttingen, Germany reveal a seasonal cycle driven by biospheric uptake. *Geochimica et Cosmochimica Acta*, *199*, 143–163. https://doi.org/10.1016/j.gca.2016.11.019

Horváth, B., Hofmann, M. E. G., & Pack, A. (2012). On the triple oxygen isotope composition of carbon dioxide from some combustion processes. *Geochimica et Cosmochimica Acta*, *95*, 160–168. https://doi.org/10.1016/j.gca.2012.07.021

Kawagucci, S., Tsunogai, U., Kudo, S., Nakagawa, F., Honda, H., Aoki, S., et al. (2005). An analytical system for determining δ^{17}O in CO_2 using continuous flow-isotope ratio MS. *Analytical Chemistry*, *77*(14), 4509–4514. https://doi.org/10.1021/ac050266u

Kelson, J. R., Petersen, S. V., Niemi, N. A., Passey, B. H., & Curley, A. N. (2022). Looking upstream with clumped and triple oxygen isotopes of estuarine oyster shells in the early Eocene of California, USA. *Geology*, *50*(7), 755–759. https://doi.org/10.1130/G49634.1

Koren, G., Schneider, L., Velde, I. R., Schaik, E., Gromov, S. S., Adnew, G. A., et al. (2019). Global 3-D simulations of the triple oxygen isotope signature Δ^{17}O in atmospheric CO_2. *Journal of Geophysical Research: Atmospheres*, *124*(15), 8808–8836. https://doi.org/10.1029/2019JD030387

Luz, B., & Barkan, E. (2010). Variations of ^{17}O/^{16}O and ^{18}O/^{16}O in meteoric waters. *Geochimica et Cosmochimica Acta*, *74*(22), 6276–6286. https://doi.org/10.1016/j.gca.2010.08.016

Mahata, S., Bhattacharya, S. K., Wang, C.-H., & Liang, M.-C. (2012). An improved CeO_2 method for high-precision measurements of ^{17}O/^{16}O ratios for atmospheric carbon dioxide: High-precision triple-isotope measurements of CO_2. *Rapid Communications in Mass Spectrometry*, *26*(17), 1909–1922. https://doi.org/10.1002/rcm.6296

Mahata, S., Bhattacharya, S. K., Wang, C. H., & Liang, M. C. (2013). Oxygen isotope exchange between O_2 and CO_2 over hot platinum: An innovative technique for measuring Δ^{17}O in CO_2. *Analytical Chemistry*, *85*(14), 6894–6901. https://doi.org/10.1021/ac4011777

Matsuhisa, Y., Goldsmith, J. R., & Clayton, R. N. (1978). Mechanisms of hydrothermal crystallization of quartz at 250°C and 15 kbar. *Geochimica et Cosmochimica Acta*, *42*(2), 173–182. https://doi.org/10.1016/0016-7037(78)90130-8

McCrea, J. M. (1950). On the isotopic chemistry of carbonates and a paleotemperature scale. *The Journal of Chemical Physics*, *18*(6), 849–857. https://doi.org/10.1063/1.1747785

McKinney, C. R., McCrea, J. M., Epstein, S., Allen, H. A., & Urey, H. C. (1950). Improvements in mass spectrometers for the measurement of small differences in isotope abundance ratios. *Review of Scientific Instruments*, *21*(8), 724–730. https://doi.org/10.1063/1.1745698

McManus, J. B., Nelson, D. D., Shorter, J. H., Jimenez, R., Herndon, S., Saleska, S., & Zahniser, M. (2006). A high precision pulsed quantum cascade laser spectrometer for measurements of stable isotopes of carbon dioxide. *Journal of Modern Optics*, *52*(16), 2309–2321. https://doi.org/10.1080/09500340500303710

Miller, M. F. (2002). Isotopic fractionation and the quantification of ^{17}O anomalies in the oxygen three-isotope system: An appraisal and geochemical significance. *Geochimica et Cosmochimica Acta*, *66*(11), 1881–1889. https://doi.org/10.1016/S0016-7037(02)00832-3

Miller, M. F., & Pack, A. (2021). Why measure ^{17}O? Historical perspective, triple-isotope systematics and selected applications. *Reviews in Mineralogy and Geochemistry*, *86*(1), 1–34. https://doi.org/10.2138/rmg.2021.86.01

Mrozek, D. J., van der Veen, C., Kliphuis, M., Kaiser, J., Wiegel, A. A., & Röckmann, T. (2015). Continuous-flow IRMS technique for determining the ^{17}O excess of CO_2 using complete oxygen isotope exchange with cerium oxide. *Atmospheric Measurement Techniques*, *8*(2), 811–822. https://doi.org/10.5194/amt-8-811-2015

Nelson, D. D., McManus, J. B., Herndon, S. C., Zahniser, M. S., Tuzson, B., & Emmenegger, L. (2008). New method for isotopic ratio measurements of atmospheric carbon dioxide using a 4.3 μm pulsed quantum cascade laser. *Applied Physics B*, *90*(2), 301–309. https://doi.org/10.1007/s00340-007-2894-1

Pack, A., & Herwartz, D. (2014). The triple oxygen isotope composition of the Earth mantle and understanding Δ^{17}O variations in terrestrial rocks and minerals. *Earth and Planetary Science Letters*, *390*, 138–145. https://doi.org/10.1016/j.epsl.2014.01.017

Passey, B. H., Hu, H., Ji, H., Montanari, S., Li, S., Henkes, G. A., & Levin, N. E. (2014). Triple oxygen isotopes in biogenic and sedimentary carbonates. *Geochimica et Cosmochimica Acta*, *141*, 1–25. https://doi.org/10.1016/j.gca.2014.06.006

Paul, D., Scheeren, H. A., Jansen, H. G., Kers, B. A. M., Miller, J. B., Crotwell, A. M., et al. (2020). Evaluation of a field-deployable Nafion$^{\mathrm{TM}}$-based air-drying system for collecting whole air samples and its application to stable isotope measurements of CO_2. *Atmospheric Measurement Techniques*, *13*(7), 4051–4064. https://doi.org/10.5194/amt-13-4051-2020

Perdue, N., Sharp, Z., Nelson, D., Wehr, R., & Dyroff, C. (2022). A rapid high-precision analytical method for triple oxygen isotope analysis of CO_2 gas using tunable infrared laser direct absorption spectroscopy. *Rapid Communications in Mass Spectrometry*, *36*(21), e9391. https://doi.org/10.1002/rcm.9391

Prokhorov, I., Kluge, T., & Janssen, C. (2019). Laser absorption spectroscopy of rare and doubly substituted carbon dioxide isotopologues. *Analytical Chemistry*, *91*(24), 15491–15499. https://doi.org/10.1021/acs.analchem.9b03316

Saenger, C. P., Schauer, A. J., Heitmann, E. O., Huntington, K. W., & Steig, E. J. (2021). How ^{17}O excess in clumped isotope reference-frame materials and ETH standards affects reconstructed temperature. *Chemical Geology*, *563*, 120059. https://doi.org/10.1016/j.chemgeo.2021.120059

Sakai, S., Matsuda, S., Hikida, T., Shimono, A., McManus, J. B., Zahniser, M., et al. (2017). High-precision simultaneous $^{18}O/^{16}O$, $^{13}C/^{12}C$, and $^{17}O/^{16}O$ analyses for microgram quantities of $CaCO_3$ by tunable infrared laser absorption spectroscopy. *Analytical Chemistry*, *89*(21), 11846–11852. https://doi.org/10.1021/acs.analchem.7b03582

Steur, P. M., Scheeren, H. A., Nelson, D. D., McManus, J. B., & Meijer, H. A. J. (2021). Simultaneous measurement of $\delta^{13}C$, $\delta^{18}O$ and $\delta^{17}O$ of atmospheric CO_2—Performance assessment of a dual-laser absorption spectrometer. *Atmospheric Measurement Techniques*, *14*(6), 4279–4304. https://doi.org/10.5194/amt-14-4279-2021

Stoltmann, T., Casado, M., Daëron, M., Landais, A., & Kassi, S. (2017). Direct, precise measurements of isotopologue abundance ratios in CO_2 using molecular absorption spectroscopy: Application to $\Delta^{17}O$. *Analytical Chemistry*, *89*(19), 10129–10132. https://doi.org/10.1021/acs.analchem.7b02853

Sturm, P., Tuzson, B., Henne, S., & Emmenegger, L. (2013). Tracking isotopic signatures of CO_2 at the high altitude site Jungfraujoch with laser spectroscopy: Analytical improvements and representative results. *Atmospheric Measurement Techniques*, *6*(7), 1659–1671. https://doi.org/10.5194/amt-6-1659-2013

Tan, Y., Kochanov, R. V., Rothman, L. S., & Gordon, I. E. (2019). Introduction of water-vapor broadening parameters and their temperature-dependent exponents into the HITRAN database: Part I—CO_2, N_2O, CO, CH_4, O_2, NH_3, and H_2S. *Journal of Geophysical Research: Atmospheres*, *124*(21), 11580–11594. https://doi.org/10.1029/2019JD030929

Thiemens, M. H., Chakraborty, S., & Jackson, T. L. (2014). Decadal $\Delta^{17}O$ record of tropospheric CO_2: Verification of a stratospheric component in the troposphere: 10 yr record of $\Delta^{17}O$ of tropospheric CO_2. *Journal of Geophysical Research: Atmospheres*, *119*(10), 6221–6229. https://doi.org/10.1002/2013JD020317

Thiemens, M. H., Jackson, T. L., & Brenninkmeijer, C. A. M. (1995). Observation of a mass independent oxygen isotopic composition in terrestrial stratospheric CO_2, the link to ozone chemistry, and the possible occurrence in the Martian atmosphere. *Geophysical Research Letters*, *22*(3), 255–257. https://doi.org/10.1029/94GL02996

Tuzson, B., Mohn, J., Zeeman, M. J., Werner, R. A., Eugster, W., Zahniser, M. S., et al. (2008). High precision and continuous field measurements of $\delta^{13}C$ and $\delta^{18}O$ in carbon dioxide with a cryogen-free QCLAS. *Applied Physics B*, *92*(3), 451–458. https://doi.org/10.1007/s00340-008-3085-4

Voarintsoa, N. R. G., Barkan, E., Bergel, S., Vieten, R., & Affek, H. P. (2020). Triple oxygen isotope fractionation between $CaCO_3$ and H_2O in inorganically precipitated calcite and aragonite. *Chemical Geology*, *539*, 119500. https://doi.org/10.1016/j.chemgeo.2020.119500

Wang, Z., Nelson, D. D., Dettman, D. L., McManus, J. B., Quade, J., Huntington, K. W., et al. (2020). Rapid and precise analysis of carbon dioxide clumped isotopic composition by tunable infrared laser differential spectroscopy. *Analytical Chemistry*, *92*(2), 2034–2042. https://doi.org/10.1021/acs.analchem.9b04466

Wostbrock, J. A. G., Brand, U., Coplen, T. B., Swart, P. K., Carlson, S. J., Brearley, A. J., & Sharp, Z. D. (2020). Calibration of carbonate-water triple oxygen isotope fractionation: Seeing through diagenesis in ancient carbonates. *Geochimica et Cosmochimica Acta*, *288*, 369–388. https://doi.org/10.1016/j.gca.2020.07.045

Wostbrock, J. A. G., Cano, E. J., & Sharp, Z. D. (2020). An internally consistent triple oxygen isotope calibration of standards for silicates, carbonates and air relative to VSMOW2 and SLAP2. *Chemical Geology*, *533*, 119432. https://doi.org/10.1016/j.chemgeo.2019.119432

Yanay, N., Wang, Z., Dettman, D. L., Quade, J., Huntington, K. W., Schauer, A. J., et al. (2022). Rapid and precise measurement of carbonate clumped isotopes using laser spectroscopy. *Science Advances*, *8*(43), eabq0611. https://doi.org/10.1126/sciadv.abq0611